

A low cost miniature PZT amplifier for wireless active structural health monitoring

Claudio Olmi¹, Gangbing Song^{*1,2}, Leang-San Shieh¹ and Yi-Lung Mo³

¹Department of Electrical Engineering, University of Houston, 77204, USA

²Department of Mechanical Engineering, University of Houston, 77204, USA

³Department of Civil Engineering, University of Houston, 77204, USA

(Received December 20, 2009, Accepted March 9, 2011)

Abstract. Piezo-based active structural health monitoring (SHM) requires amplifiers specifically designed for capacitive loads. Moreover, with the increase in number of applications of wireless SHM systems, energy efficiency and cost reduction for this type of amplifiers is becoming a requirement. General lab grade amplifiers are big and costly, and not built for outdoor environments. Although some piezoceramic power amplifiers are available in the market, none of them are specifically targeting the wireless constraints and low power requirements. In this paper, a piezoceramic transducer amplifier for wireless active SHM systems has been designed. Power requirements are met by two digital On/Off switches that set the amplifier in a standby state when not in use. It provides a stable ± 180 Volts output with a bandwidth of 7k Hz using a single 12 V battery. Additionally, both voltage and current outputs are provided for feedback control, impedance check, or actuator damage verification. Vibration control tests of an aluminum beam were conducted in the University of Houston lab, while wireless active SHM tests of a wind turbine blade were performed in the Harbin Institute of Technology wind tunnel. The results showed that the developed amplifier provided equivalent results to commercial solutions in suppressing structural vibrations, and that it allows researchers to perform active wireless SHM on moving objects with no power wires from the grid.

Keywords: structural health monitoring; wireless sensor network; amplifier; active sensing; miniature PZT amplifier.

1. Introduction

Piezoceramic materials have been actively researched in the structural health monitoring (SHM) community for decades (Chang *et al.* 2003). In general, we can categorize their application by the way we used them: passive or active. In passive mode, piezoceramic materials are used as an impedance sensor and/or vibration sensor (Naidu and Soh 2004). Data collected is typically used to perform model updating. The main benefit of passive SHM is the low speed data acquisition requirements, but the data is complex to interpret and it requires prior knowledge of the host structure dynamics. On the other hand, when used in active mode, the sensors are also the actuators, thus, while a single piezoceramic transducer actuator generates a vibration inside the structure, the remaining piezoceramic sensors in the structure monitor the energy of the propagated waveforms.

*Corresponding Author, Professor, E-mail: gsong@uh.edu

This technique has been used to monitor damage in a concrete column and a concrete 3D structure (Gu *et al.* 2007, Liao *et al.* 2008). Gu *et al.* packaged PZT (Lead Zirconate Titanate, a type of piezoceramic material) patches into a small concrete block and called them Smart Aggregate (SA). Prior knowledge of the host structure dynamics is not necessary for interpreting the data, while it is advised for the correct placement of the SAs.

While the passive use of this materials requires modeling and parameter updating to understand the health status of structures (Timothy *et al.* 2008), active SHM solely requires the total energy of the received signal, thus simplifying calculations (Song *et al.* 2007). Although the great advantages of active sensing, their use is limited by two components: the data acquisition system and the high voltage amplifier to drive the actuators. Advances in the digital design of chips are rapidly bringing the embedded data acquisition systems to the required levels. On the other hand, power requirements, cost and size of the piezoceramic amplifiers have remained constant. In the active SHM, requirements are typically set to ± 200 V with a bandwidth of 10-20k Hz. A low cost and size instrument compatible with the aforementioned requirements is typically around US\$900, and they still require connection to the power grid. There are other cheaper solutions, but with a reduced bandwidth, usually below 1k Hz, and/or positive only voltage output which are typically used for piezoceramic stack actuators, piezoceramic buzzers, or piezoceramic motors.

The use of piezoceramic materials in real sized structures has also been a challenge because of the high cost of wiring many sensors in the structures. A solution to this is the introduction of wireless sensor networks (WSN). Typical WSN divide the problem into multiple battery operated nodes. The solution works well when the PZT is used as a sensor only, or passive, but not in active mode since each node would require an amplifier to drive the piezoceramic actuators and a high speed data acquisition embedded circuit (Jeongyeup *et al.* 2005).

In this paper, a miniaturized amplifier for piezoceramic actuators has been developed to target the wireless sensor network requirements of small scale, power management and low battery requirements. Based on preliminary study and tests (Song *et al.* 2009), the minimum requirements are 6k Hz bandwidth at ± 180 V operated by a single 12 V battery. The amplifier includes an input preamplifier to allow positive only input voltages up to 3 V to drive a piezoceramic actuator from an embedded system. Two sets of power switches are included: the first to switch on and off the high voltage power supply to conserve power, and the second to switch the load connectors from the amplifier to a charge amplifier. The latter allows the use of the piezoceramic actuator to be reused as a sensor when needed. This paper is an update to the previous work done in 2008 and 2009, thus not all the unchanged material will be covered due to space limitations (Olmi *et al.* 2008, 2009).

2. Electrical design

Piezoceramic materials such as PZTs are modeled as a non-ideal capacitor in series with a voltage source that generate a charge proportional to the strain observed by the material. When used as an actuator, the PZT is driven by a large voltage to compensate for the large internal resistance.

To reduce the cost and size of current piezoceramic amplifiers, the first objective was to find commercial off the shelf (COTS) components that could perform the tasks of driving capacitive loads and of generating high voltages. For the first task, a popular solution is using Cirrus Logic (formerly Apex Microtech Inc.) high voltage operational amplifiers specifically designed for capacitive loads. The PA15FLA was chosen because it provides similar voltage and current outputs specification than

the commercial PZT amplifier chosen as a benchmark. The chosen commercial amplifier is the Mide Quickpack QPA 200 that provides 200 mA of current at ± 200 V (2011). It is important to note that the developed amplifier is not intended to compete with any commercial product, but rather to provide a solution to the portability and size demands of active wireless SHM yet to be addressed by companies.

The required current needed by the piezoceramic load can be calculated from Eq. 1 below. The method assumes that the piezoceramic load is just an ideal capacitor.

$$I_{Output(peak)} = V_{Output(peak)} \cdot 2 \cdot \pi \cdot f_{max} \cdot C_{Load} \tag{1}$$

The equation is used to find the maximum current required to drive a PZT with capacitance C_{Load} at the maximum frequency f_{max} outputting a sine wave of voltage $V_{Output(peak)}$. Since the maximum current depends on the PZT characteristics, the capacitive load value was chosen equal to the capacitance of a typical Smart Aggregate, 5n F measured at 820 Hz. Thus, given that our requirements demand an output voltage of ± 180 V and a sinusoidal excitation frequency of at least 6k Hz, the maximum current required is

$$I_{Output(peak)} = 180V \cdot 2 \cdot \pi \cdot 6000Hz \cdot 5nF = 34mA \tag{2}$$

The above value sets an approximate current target of the high voltage power supply, more importantly, the above equation provide us with power requirements of $P = V \cdot I = 180 \cdot 0.034 = 6.12W$. For the same output voltage, higher currents provide higher frequencies. For the second task, and given the previously set and discovered requirements, the F04CT power supply was chosen from EMCO High Voltage Corporation. The power supply provides 25mA at ± 200 V, or approximately 10 W of total power. The value seems at the boarder line with the requirements, but the efficiency of DC/DC switching amplifiers is at its maximum when the load requires the maximum deliverable power from it, thus providing the least amount of losses in the circuit. Fig. 1 shows the complete block diagram of the amplifier.

The input signal is first manually selected between a high voltage and a low voltage one. The first allows the user to control the amplifier using a standard BNC connector J_3 with a maximum voltage swing of $[-10, +10]$ Volts (In/Sig in the above diagram). The range is compatible with most laboratory data acquisition systems analog outputs. On the other hand, from connector J_{10} , the low voltage input is used for miniature embedded systems, which are normally capable of outputting only positive low voltage analog signals. The range is limited to $[0, 3]$ Volts (Pre). Thus, at the input of the amplifier stage (Amp), the voltage should always be in the range of $[-10, +10]$ Volts; Fig. 2 shows the electronic

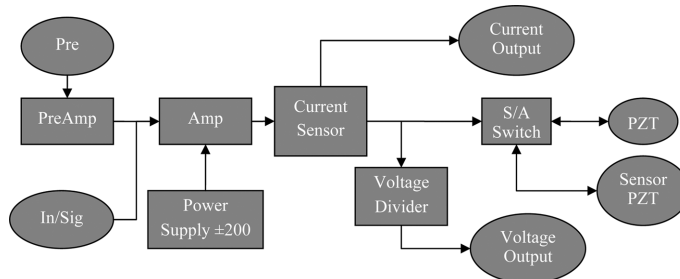


Fig. 1 Block diagram of developed piezoceramic amplifier

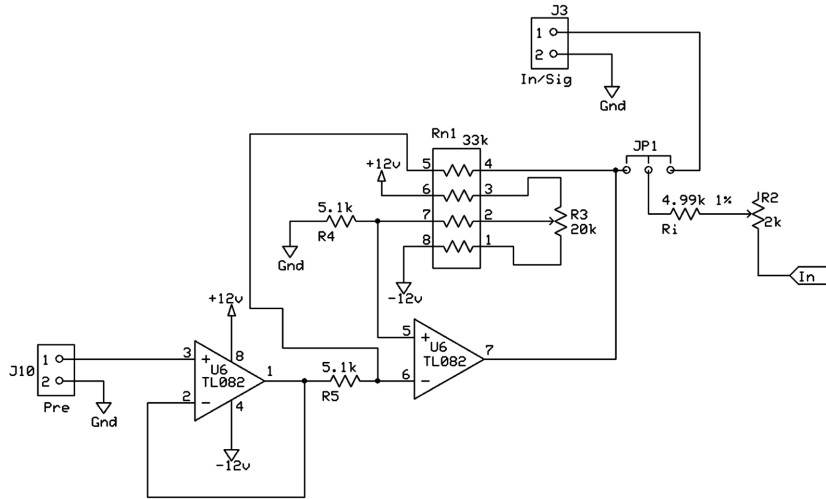


Fig. 2 Input stage with user selectable input range, 3 V or ±10 V

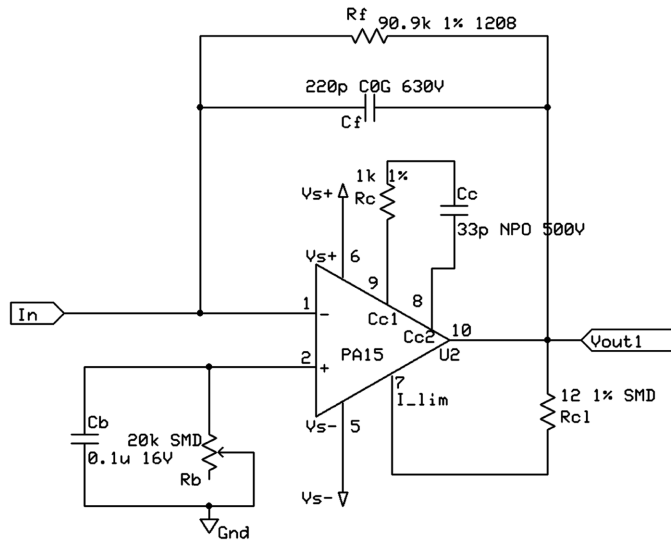


Fig. 3 Inverting operational amplifier for piezoceramic actuators

input stage.

The main amplifying circuit is a typical inverting operational amplifier which provides a constant gain of -18. The gain is negative because it is an inverting amplifier configuration and it is set by the two resistors R_f and R_i while the gain can be fine tuned by varying the potentiometer R_2 respectively shown in Figs. 2 and 3. Mathematically the amplifier is equivalent to a single pole low pass filter with a fixed gain. The capacitor and resistor, C_f and R_f , sets the pole location, while the ratio of R_f and R_i sets the gain. The transfer function of the amplifier is

$$G(s) = -\frac{1/C_f(R_i + R_2)}{2 + 1/C_f R_f} = \frac{[-9.001 \times 10^5, -6.447 \times 10^5]}{s + 1/19.996 \times 10^{-6}} \quad (3)$$

where the numerator interval correspond to the range of obtainable values for the gain using R_2 . The theoretical bandwidth is set to

$$f_c = \frac{1}{2 \times \pi \times C_f R_f} = 7.96 \times 10^3 [Hz] \tag{4}$$

Since the gain can be adjusted with potentiometer R_2 , the resulting gain change can simply be represented as

$$Gain = \frac{R_f}{R_i + R_2} = -\frac{90.9k}{4.99k + [0, 2k]} = [-13, -18.2] \tag{5}$$

At the output of the operational amplifier the signal is at a voltage of around ± 180 V. Conventional current sensing methods have to be modified to compensate for the large common mode voltage. In addition, the current to the load is generally below 25m A, which is the maximum allowed by the EMCO power supply. Fig. 4 shows the overall output monitoring circuitry. R_{10} is the current sensor, and it has a very high resistance compared to the typical current sensors because of the low output current to be monitored. R_{11} is used to compensate for the large current sensor resistor. The high common mode voltage seen by the current sensor is taken care of by the specialized chip AD629, which can handle high voltages. The current sensor circuit is followed by a voltage buffer.

To monitor the voltage applied to the piezoceramic load, a simple voltage divider in parallel with the load would be able to work, but care needs to be taken in choosing the right resistor values. Since the PZT actuator is a high impedance load, any resistor in parallel with it will have to be high enough to minimize the current taken away from the load. In this design, the current is set to $100 \mu A$. The resistors R_7, R_8 and R_1 sets a voltage divider that converts the high voltage into a $1/40$ representation.

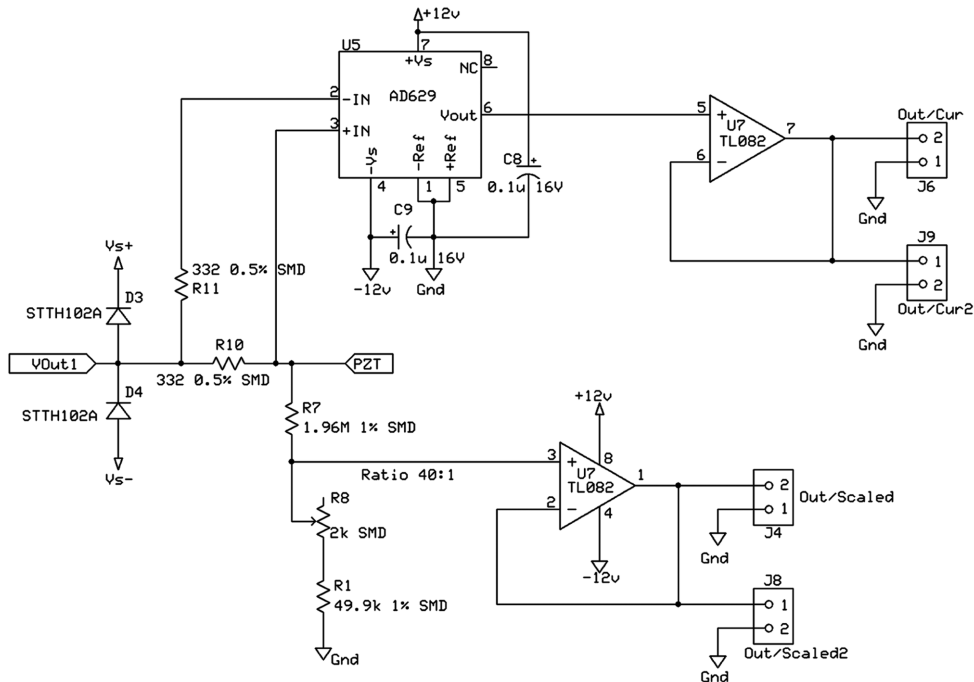


Fig. 4 Output monitoring circuit for current and voltage

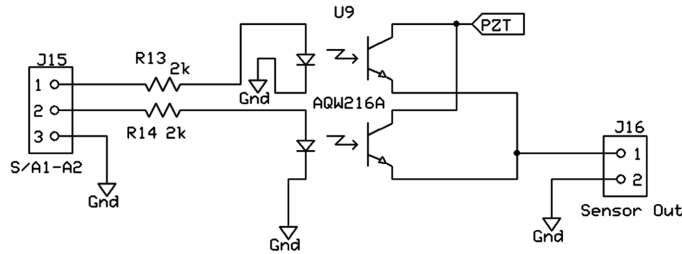


Fig. 5 Sensor/Actuator mode switch

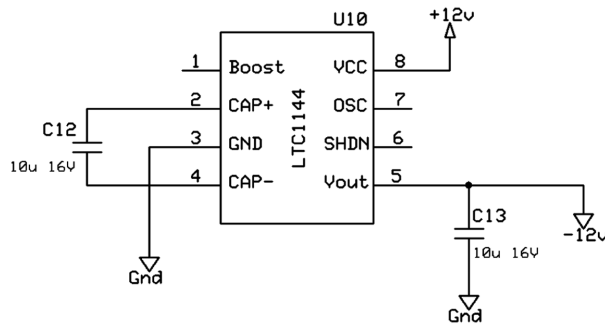


Fig. 6 -12 [V] generator from +12 [V] source

R_8 is used to tune the ratio. The scaled down voltage is then buffered using an operational amplifier.

Since piezoceramic transducers can be used as a sensor or as an actuator, an external embedded system could potentially re-route the load pins to a different circuit for sensing purposes. Fig. 5 shows the sensor/actuator mode switch. The photo-MOSFETs have an On resistance of around 70 Ohm each and they can handle high voltages up to 600 V. To further reduce their On resistance, the two MOSFETs have been connected in parallel. When the piezoceramic amplifier is not functional, the piezoceramic load is by default connected as a sensor, only after external commands the piezoceramic load is switched to actuator, thus reducing the consumption during the amplifier standby.

Lastly, to power the various operational amplifiers for output monitoring and input conditioning, it is required to have a negative supply voltage. Since the piezo amplifier is powered by a single 12 V battery, the -12 V line had to be generated. Fig. 6 shows the LTC1144 integrated circuit configured to convert the positive 12 Volt input voltage into a negative voltage supply.

3. Testing results

A printed circuit board (PCB) was designed and fabricated using an external company, while the components were manually soldered in the lab. Fig. 7 shows the final product. The high voltage power supply is the biggest component, while the operational amplifier heat sink requirements were met by just attaching a thick aluminum piece.

The total cost of the components used to assemble the amplifier was around US\$300, which is well below the cost of some of the smallest commercial amplifiers. In addition, the use of a single 12 V battery allows users to be away from the power grid and recharge the battery with conventional means.

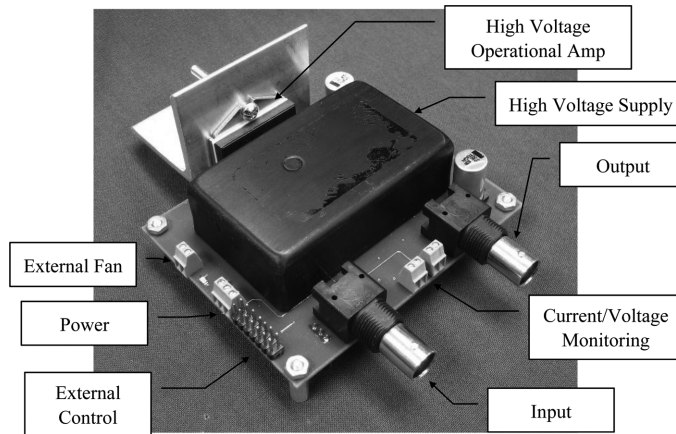


Fig. 7 Developed piezoceramic amplifier

Before introducing the results, the amplifier was adjusted to provide the correct output voltage ratio and gain, respectively 1/40 and -18. The conducted tests were all done in an indoor university settings, thus the amplifier was not tested in any extreme environment. The load used for the tests was a Smart Aggregate with a capacitance of 5.4n F.

The amplifier was tested for its effective bandwidth using a chirp signal from 1 Hz to 10k Hz, providing enough data to plot the system frequency response: Fig. 8 shows the frequency response

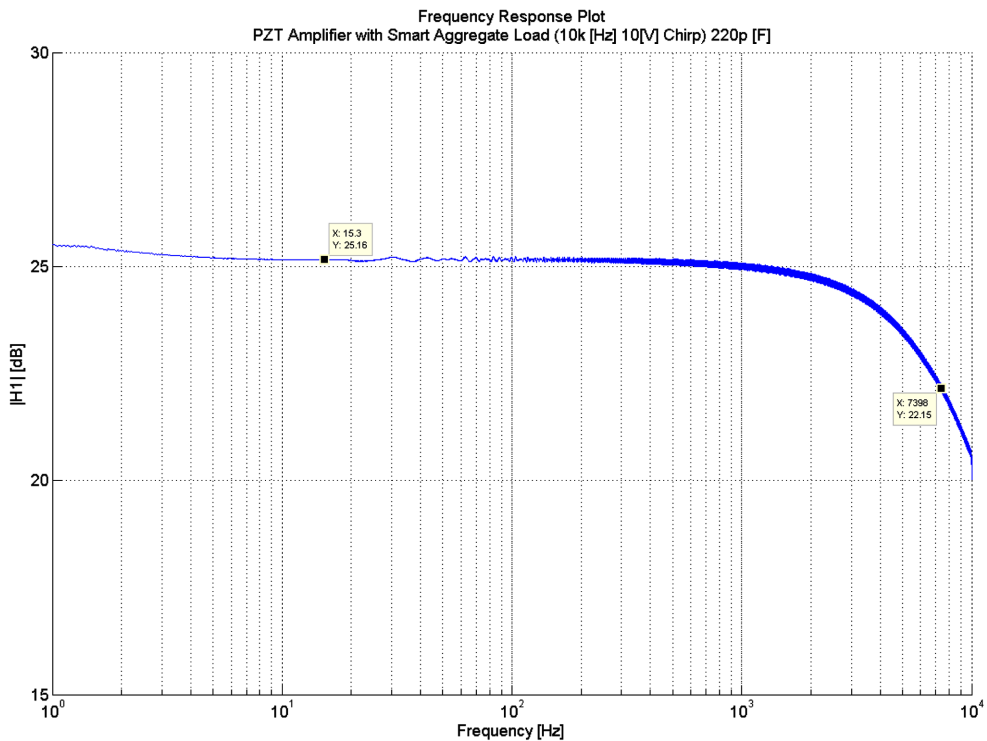


Fig. 8 Frequency response of output scaled voltage vs. input voltage

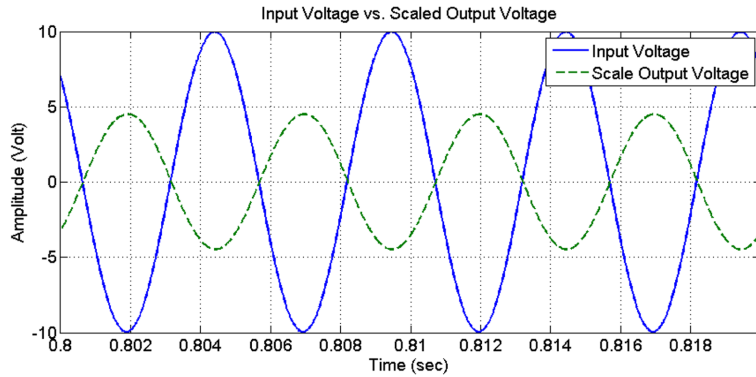


Fig. 9 Time domain comparison

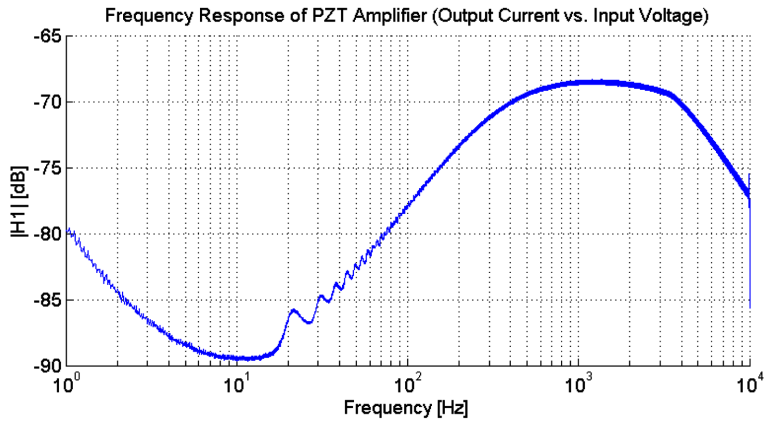


Fig. 10 Frequency response of output current vs. input voltage

plot. From the figure, the bandwidth at -3 dB is approximately 7.3k Hz which is similar to the calculated one in Eq. 4.

When looking at the time domain plot in Fig. 10, we can see that we have the expected change in phase, negative gain, and no major distortion in the signal. The result confirms Eq. 5 negative gain.

The amplifier provides both voltage and current monitoring. Fig. 10 shows the frequency response of the input voltage versus output current to the PZT actuator. Although the absolute value of the magnitude does not provide useful insights, the relative value is. In fact, from the figure we can proof equation

$$I_{output} = C_{pzt} \frac{dV(t)}{dt} = C_{pzt} \times SlewRate = C_{pzt} \times (2 \times \pi \times f) \times V_{Peak} \tag{6}$$

that says that increases in actuation frequencies produces an increase in current requirements for the same excitation voltage, or that the maximum required current occur when the slew rate is at its maximum. From the figure we can identify the low current region at around 15.3 Hz. The current output increases until the maximum bandwidth of the amplifier identified from Fig. 8. Then, because the current is also proportional to the voltage applied to the load, the current output reduces. In other words, the increase of the frequency effect on the output current is lower then the decrease effect of the

Table 1 Effect of power switch to the required current

Sleep switch state	Input signal	Output current m[A]	Input current m[A]
OFF	Disconnected		24
ON	Disconnected		499
ON	100 Hz	1.28	506
ON	1000 Hz	8.85	557
ON	5000 Hz	29.50	835
ON	10000 Hz	25.00	1047

output voltage.

With the use of a bench multi meter, the current requirements for the amplifier were recorded at different frequencies using a single sinewave input. Table 1 lists the results. As the frequency of the input sinewave increases, the output current increases up to the bandwidth of the amplifier 7.3k Hz. When the output voltage decreases at frequencies above the amplifier cut off value, the output current decreases. In a possible wireless application implementing the active SHM, the amplifier would transmit for around 5 seconds every month at a maximum of 1 A, while the rest of the time would be in stand by at 24m A. Thus, the projected power requirements of the amplifier in Watt/ Month using the values from Table 1 would be around

$$P = A_{Month-Avg.} \times V_{Batt.} = \left(\frac{5 \times 1 + ((60 \cdot 60 \cdot 24 \cdot 30) - 5) \times 0.024}{60 \cdot 60 \cdot 24 \cdot 30} \right) \times 12 = 288.02 [\text{mW}] \quad (7)$$

A five-second transmission period is enough to run one complete chirp signal. The result is used to calculate the structure health every month. The current consumed during stand by mode is the most important to optimize in future work since it represents 99.99% of the total power requirement calculated in Eq. 7. A typical 1.2 Amp/hour lead acid 12 Volt battery would be able to power the amplifier for around 50 hours without energy harvesting.

4. Applications

The above tests showed that the new PZT amplifier has similar characteristics, in bandwidth and output voltage, as the Mide Quickpack QPA 200 commercial amplifier, but the developed amplifier has to be tested in real applications and its performance compared with a laboratory commercial amplifier. For the following test, an aluminum beam was used and its vibration controlled using a previously designed sliding mode feedback controller. Using a commercial amplifier (ACX QuickPack) and a dSpace data acquisition system, the beam was first excited to its first natural frequency and then its vibration controlled. Fig. 11 shows the experiment setup.

Figs. 12 and 13 above shows the resulting control action, thick line, and the uncontrolled one from respectively, the commercial amplifier and the developed one. Both are capable of reducing considerably the vibration of the beam in less than 10 seconds. The comparison between the controlled actions of the two amplifiers is shown in Fig. 14, where it is clear that the two amplifiers behave similarly. The difference in amplitude is due to the difference in the amplifier gains, the commercial one has a gain of -20 compared to the -18 of the developed one. Additionally, there is a 0.11 seconds constant delay, or phase, between the two curves. The phenomenon might be caused by the amplifier output



Fig. 11 Vibration control of an aluminum beam experiment setup

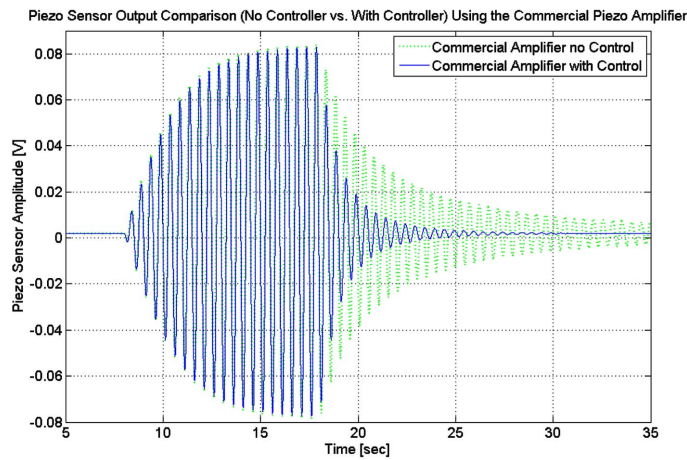


Fig. 12 Vibration control of an aluminum beam using commercial amplifier

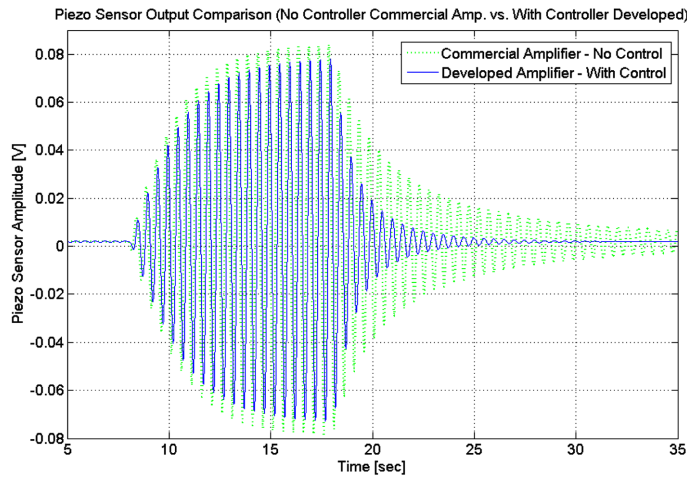


Fig. 13 Vibration control of an aluminum beam using developed amplifier

voltage electronics, however further work to identify the issue will be performed in the future.

Although vibration control of a beam using our developed piezo amplifier demonstrates the

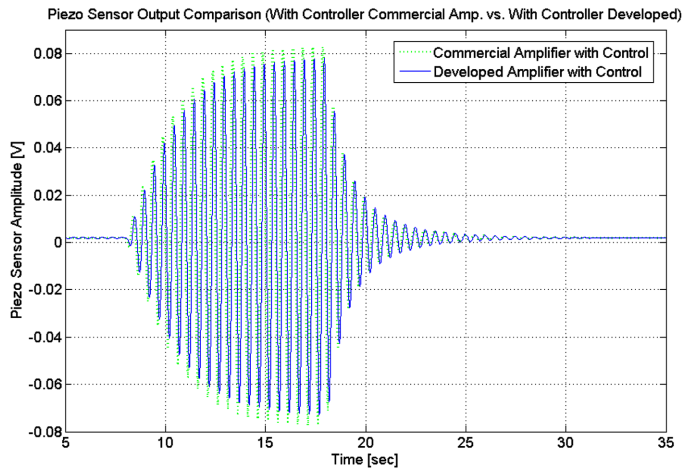


Fig. 14 Comparison of control action between the commercial amplifier and the developed one

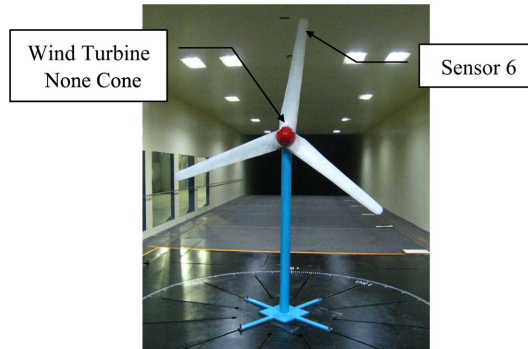


Fig. 15 Wind turbine inside the wind tunnel facility at HIT

comparable effectiveness of in laboratory applications, the ultimate target purpose is wireless active SHM. In this part of the results, the amplifier was used to perform SHM on a wind turbine blade in the wind tunnel testing facility at Harbin Institute of Technology (HIT) in China (Bosko 2009). The wind blade was equipped with 6 piezoceramic patches embedded and mounted on the surface. During the dynamic test, a 1 mm cut on the blade perpendicular to the long direction was made to represent damage. Additionally, the cut was deepened by another 1 mm to represent increased damage. Fig. 15 shows the wind turbine installed in the HIT wind tunnel.

The wireless system was designed to produce a chirp signal through the PZT actuator and simultaneously to acquire the data from the sensor nodes. The sequence of events of the actuator node were: activate the amplifier using the sleep input pin, wait 1 second to stabilize the output, generate the chirp signal between 1 to 2000 Hz, and finally set the amplifier in standby. All the nodes were built using a MSP430 microcontroller paired with a CC2500 radio transceiver and two AA batteries. In addition, the actuator node had a bigger 12 V battery and the developed amplifier. The wireless nodes were installed inside the nose cone of the wind turbine as shown in Fig. 16.

Fig. 17 shows the PZT amplifier mounted in the nose cone of the wind turbine before the wireless nodes are installed. The wind tunnel generated set wind speeds of 0, 8.6 and 10 m/s. For each wind speed, the wireless active SHM system collected a data set.

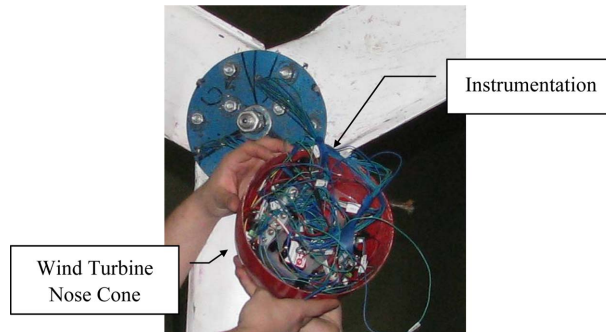


Fig. 16 Instrumentation mounted inside the turbine nose cone

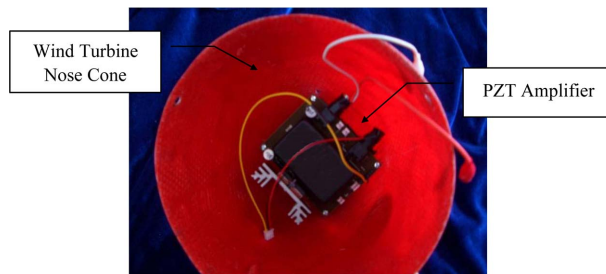


Fig. 17 Piezo amplifier mounted in the wind turbine nose cone

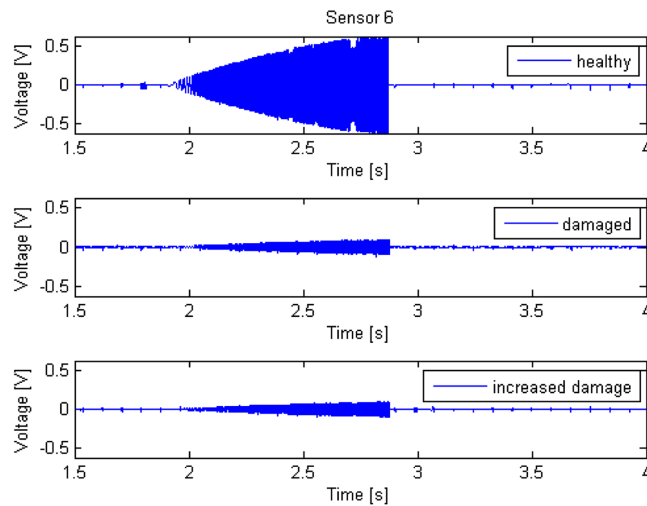


Fig. 18 Sensor 6 time domain response for the 3 cases: healthy, damaged, increased damage

For limited space purposes, only one node, or sensor, time domain plot will be shown and analyzed. Fig. 18 shows the response comparison in time domain for the healthy, the damaged and the increased damaged cases. The constant amplitude chirp signal generated by the actuator is received with some losses by sensor 6, which is surface mounted and located close to the end of the wind blade. If we take the healthy state as the reference amplitude, the damage in the blade reduces the amplitude of the received wave. By increasing the severity of the damage, there is an additional small reduction of amplitude. The small difference between the damaged and increase damage case

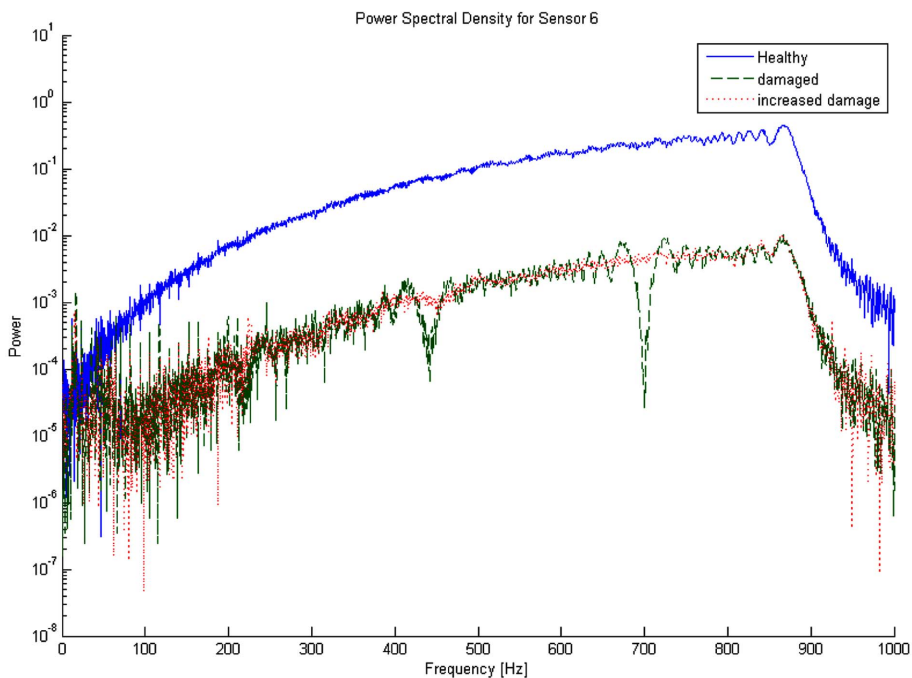


Fig. 19 Power spectrum for the 3 cases: healthy, damaged, increased damage

is due to the wave propagation in the blade. The actuator wave travelling on the surface of the blade was already attenuated by the first damage, while the embedded wave propagation was not. An increased damage on the surface did not produce a large change in the sensor amplitude because the amplitude received was already low.

The same concept is visible in Fig. 19, where energy is compared among the three cases.

The aforementioned results of the wind turbine SHM test proved the efficiency and suitability of the developed amplifier. Moreover, thanks to its portability, it allowed performing wireless active SHM on a moving object. With conventional power grid connected amplifiers the test may not have been possible.

5. Conclusions

A PZT amplifier was developed to facilitate the transition of active structural health monitoring from laboratory to real wireless applications in engineering structures. Results showed that the amplifier is comparable to the Mide Quickpack QPA 200 commercial amplifier in the frequency bandwidth of interest, but in addition, the developed amplifier is capable of functioning using a single 12 V battery and capable of running in stand by mode to save power. Currently the amplifier is contained in a space no larger than 15 in³ without the battery and the fan. The approximate component price for low quantities is around US\$300. Tests were conducted in two specific applications: vibration control of an aluminum beam, and wireless active SHM of a wind turbine blade. In the first test, it was shown that the developed amplifier provided equivalent results to commercial solutions to suppress vibrations. In the second test, the developed amplifier allowed the

researchers to perform active wireless SHM on a moving object with no power wires.

In real applications, the amplifier would be out of stand by mode only for a short period of time, just enough to output the chirp signal. Thus, future work will focus on further improving the standby power consumption and decrease the board size. Moreover, since the circuit calculations did not include the tolerance of each component, a sensitivity analysis will be performed. The replacement of the lead acid battery with a more modern lithium polymer battery and the addition of an integrated battery charger compatible with solar panels or other types of alternative energy sources would bring the amplifier one step closer to field use in wireless structural health monitoring.

Acknowledgements

This research was supported by a grant from the State of Texas's Norman Hackerman Advanced Research Program (No. 01980) and NSF awards (No. CNS 0832089 and No. CMMI 0724190).

References

- Chang, P.C., Flatau, A. and Liu, S.C. (2003), "Review paper: health monitoring of civil infrastructure", *Struct. Health Monit.*, **2**, 257-267.
- Naidu, A.S.K. and Soh, C.K. (2004), "Damage severity and propagation characterization with admittance signatures of piezo transducers", *Smart Mater. Struct.*, **13**(2), 393-403.
- Gu, H., Olmi, C. and Mo, Y.L. (2007), "Structural health monitoring of a concrete frame structure using piezoceramic based smart aggregates", *Proceedings of the World Forum on Smart Materials and Smart Structures Technology*, Chongqing and Nanjing, China.
- Liao, W.I., Gu, H., Olmi, C., Song, G., Mo, Y.L. and Loh, C.H. (2008), "Structural health monitoring of a concrete column subjected to shake table excitations using smart aggregates", *Proceedings of the Earth and Space*, San Diego.
- G.S.O. Timothy, P. Gyuhae, M.F. Kevin, and R.F. Charles, (2008), "Development of an extremely compact impedance-based wireless sensing device", *Smart Mater. Struct.*, **17**(6).
- Song, G., Olmi, C. and Gu, H. (2007), "An overheight vehicle - bridge collision monitoring system using piezoelectric transducers", *Smart Mater. Struct.*, **16**(2), 462-468.
- Jeongyeup, P., Chintalapudi, K., Govindan, R., Caffrey, J. and Masri, S. (2005), "A wireless sensor network for structural health monitoring: performance and experience", *Proceedings of the 2nd IEEE workshop on Embedded Networked Sensors: IEEE Computer Society*.
- Li, P., Song, G., Zheng, R. and Mo, Y.L. (2009), "Piezo-based wireless sensor networks for civil structural health monitoring", *Proceedings of the 1st International Postgraduate Conference on Infrastructure and Environment*, Hong Kong.
- Olmi, C., Song, G. and Mo, Y.L. (2008), "Development of a portable and low cost power amplifier for piezoceramic actuators", *Proceedings of the 4th International Workshop on Advanced Smart Materials and Smart Structures*, Tokyo, Japan.
- Olmi, C., Song, G. and Mo, Y.L. (2009), "Develop a mini-scale amplifier for piezoceramic active sensing devices for civil structural health monitoring", *Proceedings of the 1st International Postgraduate Conference on Infrastructure and Environment*, Hong Kong, China.
- Mide, "Quick pack hi voltage piezo amplifier", <http://www.mide.com/>, 2011.
- Bosko, G. (2009), "PZT based embedded systems for teaching engineering concepts and wireless structural health monitoring of wind turbine blades", in Cullen College of Engineering Dept. of Mechanical Engineering Houston: University of Houston.